ORIGINAL ARTICLE

Seismotectonic model of High-Middle Atlas Junction (Morocco) derived from earthquake focal mechanism and stress tensor analysis

Lahcen El Moudnib[1] · Youssef Timoulali[1] · Abderrahime Nouayti[1] · Mohammed El Abbassi[2] · Mustapha Bouka[1] · Nordine Nouayti[3] · Nadia Mhammdi[1]

Abstract

In this study, we attempted to derive a seismotectonic model for the High-Middle Atlas Junction area, in the central part of Morocco, by determining new earthquake focal mechanisms and tectonic stress tensor parameters. For that, we have analyzed high-quality seismic waveform data of moderate earthquakes that were collected by local broadband seismological networks between the time period from 2008 to 2014. The focal mechanisms of well-relocated earthquakes were determined using the P-wave first-motion polarities that were retrieved from the earthquake seismograms. The tectonic stress parameters were then inferred by applying a stress tensor inversion to the calculated focal mechanisms. The results that we found show that most earthquakes are characterized by predominant pure reverse faulting to reverse faulting with a minor strike-slip component. The average trend of P- and T-axes is $223.94°\pm95.6°$ and $17.68°\pm13.02°$, respectively, and the average plunge of P- and T-axes is $183.02°\pm95.22°$ and $56.32°\pm28.41°$, respectively. The estimated stress tensor parameters, describing the principal stress directions show that the axis of $\sigma1$ has the trend of $178.0°$ and dipping southward of $2.0°$ and an axis of $\sigma2$ has the trend of $268.0°$ and dipping westward of $3.0°$, indicating that both of $\sigma1$ and $\sigma2$ axes are sub-horizontal. The third stress axis, $\sigma3$, has the trend of $46.0°$ and the plunge of $87.0°$, and tends to be sub-vertical. The stress shape ratio, R, is equal to 0.61 in the whole area. These results strongly suggest that the reverse-faulting regime is predominant over the study area, and the P-axes and the stress orientations are steeply consistent with the GPS velocities field pattern derived from recent geodetic models. The seismotectonic model proposed in this study is consistent with the NW–SE displacement vector of the Nubia plate with respect to Eurasia plate and currently accommodating the central High Atlas tectonic deformation system, enhancing the slight crustal shortening process at the northern active tectonic boundary of the study area.

Keywords Seismotectonic model · Earthquake relocation · First motion · Focal mechanism · Stress inversion · HMAJ area

Introduction

The Moroccan Atlas chain is located in the northern west of Africa continent and defined by the junction between Rif mountains cordillera in the north and African Sahara plateau in the south. This narrow intracontinental chain has a general trending ENE–WSW, except the E–W and NNE–SSW trending of the eastern High Atlas and the Middle Atlas, respectively (Fig. 1). Their global geodynamics is conditioned by the relative motion of Nubia plate towards the Iberian Peninsula with a NW–SE trend at an approximate rate of 4.5 mm/year (Serpelloni et al. 2007; Buforn et al. 1995, 2004; Stich et al. 2006). For instance, the geodetic model derived from GPS data shows that the tectonic motion velocities have a clockwise rotation of the Nubia plate with respect to Iberia peninsula and are steeply consistent with

✉ Lahcen El Moudnib
lahcen.elmoudnib@is.um5.ac.ma

1 Geophysics and Natural Hazards Laboratory, Scientific Institute, Geophysics, Natural Patrimony and Green Chemistry Research Center GEOPAC, Mohammed V University in Rabat, Rabat, Morocco

2 Geology Department, Faculty of Science, Mohammed V University in Rabat, Rabat, Morocco

3 Applied Sciences Laboratory, Water and Environment Management Team, National School of Applied Sciences, Abdelmalek Essaadi University, Al Hoceima, Morocco
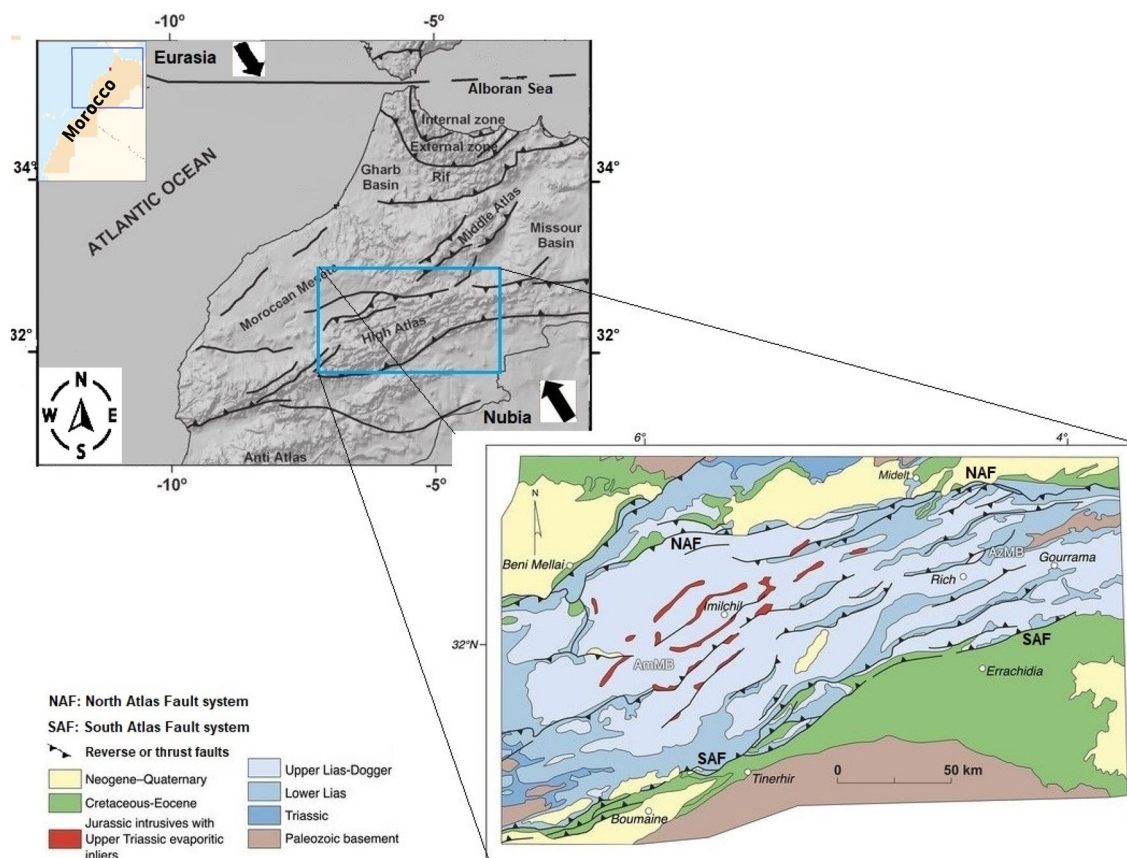
Fig. 1 Simplified tectonic model of HMAJ area (Morocco) indicating geological setting. Large black arrows indicate the convergence direction of the Nubia and Eurasia plate (from Dooley and Hudec 2020)

the oblique convergence of two plates (Vernant et al. 2010; Koulali et al. 2011).

The regional geodynamic process affected almost all structural domains of Morocco and attested by historical and instrumental seismicity along the geological structures in central and northern parts of Morocco, except the south of Morocco which is considered as an aseismic zone (Cherkaoui et al. 2012). In particular, the tectonic activity in the Moroccan Atlas is related to an intense seismicity which is concentrated along NNE–SSW trend, and reflected by some moderate earthquakes, which occurred during the last century, with magnitude ranging from 5 to 6 (Medina 2008). On the scale of the area of High-Middle Atlas Junction (HMAJ), the seismicity appears to be largely diffuse and generally moderate in size (Figs. 2 and 3).

Despite the previous seismotectonic studies of different Morocco's structure domains (Medina et al. 1991; Medina 2008; Bensaid et al. 2011; Martin et al. 2015), few earthquake focal mechanisms were investigated beneath the seismogenic zone of HMAJ area, and therefore the state of tectonic stress field, deduced from compressional forces, was poorly known. In fact, Available focal mechanism solutions determined by some agencies (USGS,

Harvard, IGN, IAG, MED, GFZ) and seismotectonic studies (Medina et Cherkaoui 1991; Medina 2008; Bensaid et al. 2011; Martin et al. 2015) using moment tensor inversion or first motion polarities are not sufficient to infer a seismotectonic model beneath the region of interest, since the Atlas is not considered as a significant seismic area, by few seismologists, in comparison to the Rif and Alboran regions, because of lack of stations covering this area at this time (Medina and Cherkaoui 1991).

Determination of the tectonic stress parameters based on the inversion of sets of earthquake focal mechanisms has been investigated by several authors (Angelier 1984; Gephart and Fortsyth 1984; Michael 1984) and has been involved to characterize the seismotectonic models in many seismogenic areas around the world (Sherif et al. 2021; Mutlu 2020; Abdulnaby et al. 2016). In fact, by knowing the state of stress in the Earth's crust, it is important to understand the mechanics of earthquakes and the mechanisms of regional deformations. The stress parameters at seismogenic zones with fractures that do not outcrop at the surface generally cannot be measured directly. Nevertheless, the trending and the plunging angles representing the orientation of the principal stress axes can be constrained from the focal

Fig. 2 Seismicity map of central and northern parts of Morocco (M > 1) and surrounding areas for the period 1900–2014 (from IS-UM5, CNRST and IGN combined catalogue), which R (Rif), MA (Middle Atlas), EM (Eastern Meseta), WM (Western Meseta), EHA (Eastern High Atlas), CHA (Central High Atlas), WHA (Western High Atlas), AA (Anti-Atlas) are the structural domains of this part of Morocco. Thick white square indicates the area of interest
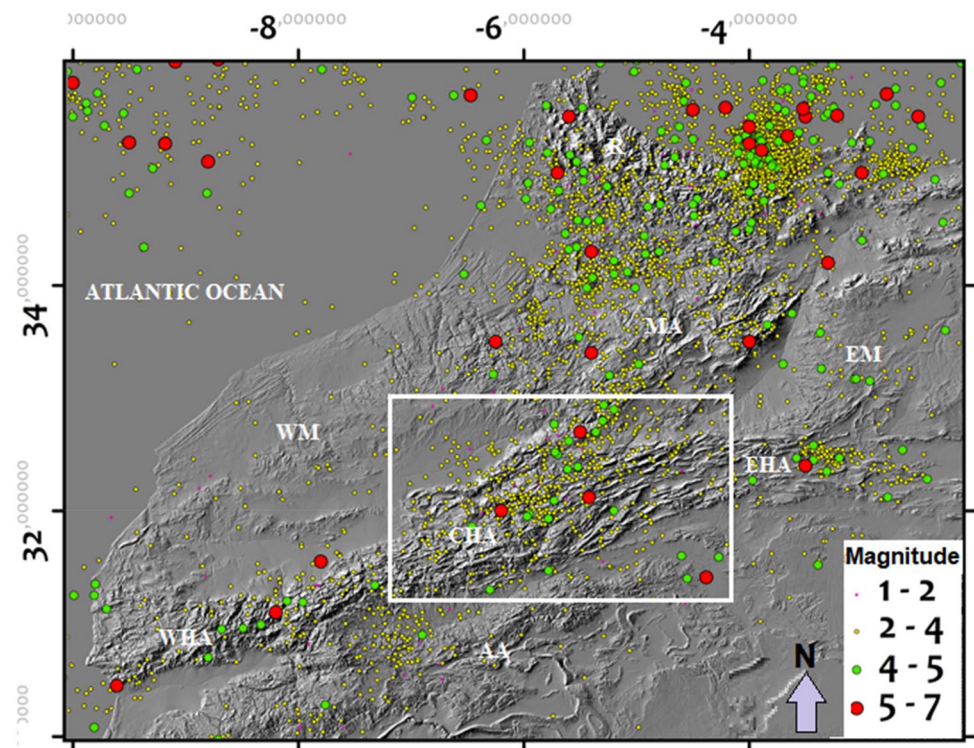
mechanisms of small magnitude earthquakes occurring in the study region.

The purpose of this paper was to develop the present-day seismotectonic model beneath the HMAJ area by analyzing moderate local earthquakes for focal mechanism solutions and stress tensor parameters determination, based on well-constrained seismic data collected during seven years of continuous seismological station recording. The obtained results are compared with the available neotectonic and seismotectonic datasets and with recent geodetic model.

Seismotectonics and geological settings

Tectonics and geological framework

The collision of the African and Eurasian lithospheric plates governs the geomorphology of Morocco (Jacobshagen et al. 1988). Indeed, the Atlas mountains, which are an active intracontinental mountain system composed of two Mesozoic rift systems, are currently accommodating the NNW–SSE Africa-Iberia convergence and are being inverted as a result of the Cenozoic-to-present convergence between Eurasia and Africa and being uplifted at a rate of ~2 mm/year since the Middle Eocene, forming this range of mountains (Jacobshagen et al. 1988; Medina and Cherkaoui 1991; Morel et al. 2000; Stich et al. 2006): (1) The Moroccan High Atlas system that runs approximately EN–EWSW to E–W, and (2) the Moroccan Middle Atlas

system that trends from NNE–SSW to NE–SW and merges into the inter-plate Betic-Rif Mountains (Fig. 1).

By the late Hercynian tectonic process, the Atlas rift was developed during the extensive phase of the basin in the Triassic period. This deformation phase formed several structural elements such as NE–SW- to E–W-trending faults and enabled the intrusion of alkaline basaltic rocks from the Upper Triassic to the Lower Jurassic. In the early Cretaceous period, the intracontinental Atlas rift underwent a tectonic inversion, moving from an extensional to a compressional regime.

The mountain ranges of both the High Atlas and the Middle Atlas, as we know them today, was molded during the alpine orogeny (Missenard 2007). It is worth mentioning that the Moroccan High and Middle Atlas do not have deep roots. Recent crustal and the upper mantle structural studies of Atlas system, from seismic ambient noise and surface-wave seismic tomography (Palomeras et al. 2017) and active seismic reflection experiment (Ayarza et al. 2014), reveal the presence of a moderate crustal thickening with Moho depth greater than 35 km and around 31 km in the central High Atlas and Middle Atlas, respectively. Seismic anisotropy derived from S and SKS splitting observations indicate polarizations predominantly sub-parallel to the trend of the central high Atlas Mountains (Lee et al. 2022; Lee et al. 2021). This could be developed by the possible NE–SW channeling of mantle flow responsible of low-velocity anomalies revealed by analyzing teleseismic data using seismic tomography
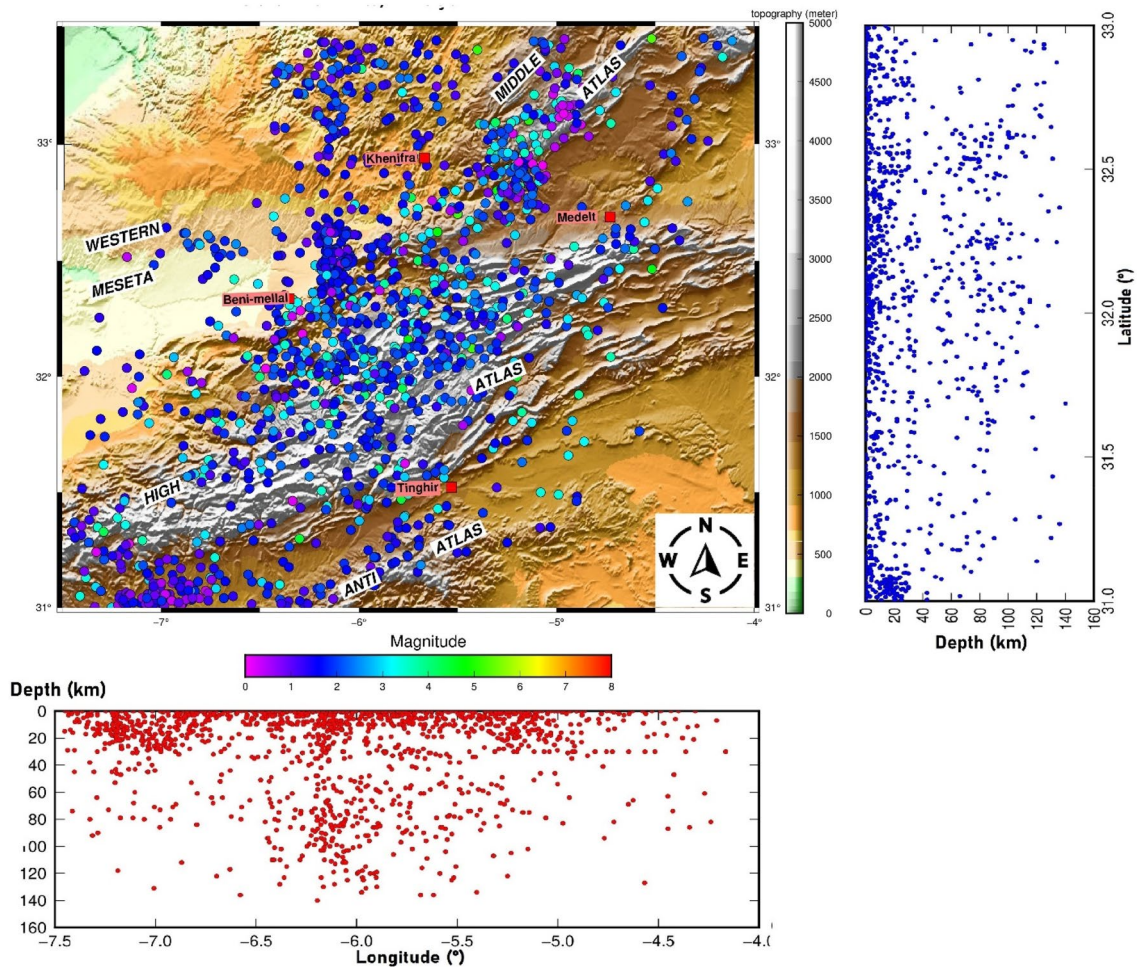
Fig. 3 Seismicity map of the area of study showing spatial distribution of all size-magnitude earthquakes (4190 events) beneath and around the study area (from IGN, CNRST, and IS-UM5). Colors of epicenter circles are proportional to earthquake magnitudes as indicated in the magnitude scale bar. Vertical distribution of earthquakes is shown in the hypocenter cross-sections along N–S (fixed longitude) and W–E (fixed Latitude)

and receiver functions (Bezada et al. 2014; Palomeras et al. 2014; Miller et al. 2013).

Further southwest, beneath western High Atlas, the Moho depth reaches an average depth value of 34 ± 5 km obtained from the inversion of teleseismic receiver functions (Spieker et al. 2014). Cross-section images of 3D velocity structure model (Timoulali et al. 2019) show a maximum crust depth of 36 km in the same region of study. However, the Atlas orogen reaches high altitudes, but the upper brittle crustal shortening is weak (Makris et al. 1985). This suggests that the orogeny of these dominant peaks is not only the cause of the crustal shortening (Frizon de Lamotte et al. 2004), which related to compression within the Nubia plate, closing the rift beneath the Atlas system. It would also be due to the tectono-sedimentary phases by detachment levels. The activation of the reverse-faulting system, originating from the Triassic–Liassic rift, would have resulted in detachments, at quite important depth, that formed surface deformation.

The N–S-directed compression, that is still current, affecting the High Atlas chain is clearly displayed by E–W-trending active reverse faulting along its borders at north and south (Sebrier et al. 2006). Faulting systems, resulting from the extensional regime of the rift, have modeled the main orientation of the Atlas Mountains as well as the formation of multiple synclinal and anticlinal folds (Laville and Piqué 1992 ; Frizon de Lamotte et al. 2000 ; Teixell et al. 2003).

The Central High Atlas domain in particular is constituted by the Paleozoic basement and covered by a thick Mesozoic layer. This Atlas domain is bordered in the north by the North Atlas fault system (NAF) and in the south by the South Atlas fault system (SAF) (Fig. 1). This domain is characterized by horst and graben systems, initially developed as a subsiding basin. The Jurassic sediment cover was controlled by both local tectonic and global geodynamic factors. The faulting system influencing the geodynamic evolution of the Central High Atlas (Ait Brahim and Chotin 1984; Morel

et al. 2000) is characterized by: (1) the NE–SW trending of most frequent faults which were developed at the upper Cretaceous (Fig. 1) and was reactivated as reverse faults with a left-lateral strike-slip component. The ENE–WSW faulting system dominated the Mesozoic evolution of the Central High Atlas and was reactivated later during the Neogene and Quaternary times. (2) the transverse NW–SE and NNW–SSE faulting systems developed as reverse thrusts with a left-lateral strike-slip component. (3) the E–W faulting system in the Central High Atlas is succeeded to the tectonic structures during Hercynian orogeny. These faults were the results of the Alpine evolution of the High Atlas range which developed as reverse and thrust faults with a right-lateral strike-slip component.

Seismicity and seismotectonics

Morocco is characterized by moderate seismicity along the active tectonic structures and blocks mainly. Global distribution of the epicenters shows that most earthquakes are occurring at the offshore and the onshore areas of the northern part of the country, which is evidence since these areas are close to the inter-plate collision zone (Fig. 2).

Compared to other seismically active parts of different structural domains of Morocco, Atlas domain is considered as a significant seismicity area after the Rif domain since this latter is close to high tension continental collision zone. However, scares and diffuse seismic activity is still observed in the Atlas chain region over the three distinct Atlas blocks (Middle, High and Anti-Atlas) (Fig. 2). To the south, in the Sahara region, generally no seismic activity is observed (seldom seismic events are reported, but with inaccurately hypocenter location) and, the seismicity decreases along the eastern High Atlas (Cherkaoui et al. 2012). Seismic events are generally caused by local active tectonic deformations and by the major faults related to regional geodynamic process of the oblique NW–SE convergence between Nubian and Eurasian plates at a rate of ~ 5 mm/year.

As a consequence, the regional distribution of the Atlas earthquake epicenters appears to emphasize a rugged NE–SW trend, which is sub-parallel to the Middle Atlas chain, but oblique to the WSW–ESE orientation of the High Atlas. Particularly, the HMAJ area was characterized by a relatively large amount of seismic activity at various depths (Fig. 3). In fact, hypocentral depths are less than 30 km for most events, despite some events having been produced and distributed by depth between intermediate (greater than 30 km) and large depth (greater than 70 km), particularly on the reverse faults of the central High Atlas.

On the basis of the magnitude size, the major seismicity is characterized by moderate earthquakes in which many of them have a local magnitude ranging between 4 and 6. In

few last decades, famous moderate earthquakes caused low-to-great damage as in Agadir (1731, 1960), Souk El Khemis (1957), Essaouira (1988), Rissani (1992) and lately in Midlet (2019), but the famous and largest earthquake ever recorded within the Atlas domain corresponds to the destructive 29 February 1960, Agadir earthquake, with 5.7 as a magnitude, which leaving 12,000 dead, 25,000 injured with a heavy damage (Bensaid et al. 2011; Medina 2008; Medina et al. 2011; Medina et al. 2021).

Present-day convergence between two lithospheric plates, Nubian and European, appears to be N–S to NNW–SSE oriented, as revealed by the compression axis derived from available earthquake focal mechanisms (Medina and Cherkaoui 1992; Gomez et al. 1996) and from previous neotectonic studies (Ait Brahim and Chotin 1984; Bernini et al. 2000). Throughout the Atlas chain, many authors have reported recent Plio-Quaternary tectonics reflected by flexures, folds and faults (Mridekh et al. 2000). This recent tectonic activity is carried out within the framework of the state of the tectonic stress characterized by compression trending NW–SE to NNE–SSW which is also found in the rest of the High Atlas (Morel et al. 2000). This tectonic regime is currently continuing, as shown by the earthquake focal mechanisms that occurred last decades in and around the High Atlas central. The southern part of the Middle Atlas shows above all compressive structures, the most important of which is the Aït Oufella fault, which was reactivated in the Plio-Quaternary as an inverse fault with a sinistral component (Medina and Cherkaoui 1991, 1992).

Data and methodology

Data acquisition and seismic experiments

High-quality seismic waveform data were recorded in the permanent and temporary seismological networks deployed in central and northern parts of Morocco (Fig. 4). The temporary seismic arrays were implemented in the frame of scientific collaboration between Scientific Institute, Mohammed V University of Rabat, Morocco and, USA and European Universities (Spain, Germany, and UK), included the TM (TopoIberia-Morocco 2007–2014), PM (Picasso-Morocco 2009–2012), MM (Morocco-Münster 2010–2012), and MB (Morocco-Bristol 2010–2012) experiments. These latter enabled to reduce considerably the data gap and to cover reasonably good all structural domains, and particularly the entire seismic active areas.

The equipment of the permanent seismic network deployed in Morocco and belonging to the WM Mediterranean network consist of STS2 broadband sensors coupled with Quanterra Q330 and EarthData PS6-24 24bytes digital dataloggers. Almost all the equipment used in the

Fig. 4 Map of seismic stations showing distribution of permanent (blue triangles, operated by IS and ROA) and portable (red, pink, brown and green triangles, operated, respectively, by the TopoIberia group, PICASSO, Munster, Bristol and Morocco (IS) teams) seismic broadband stations in central and north of Morocco. The red box frames the area of study
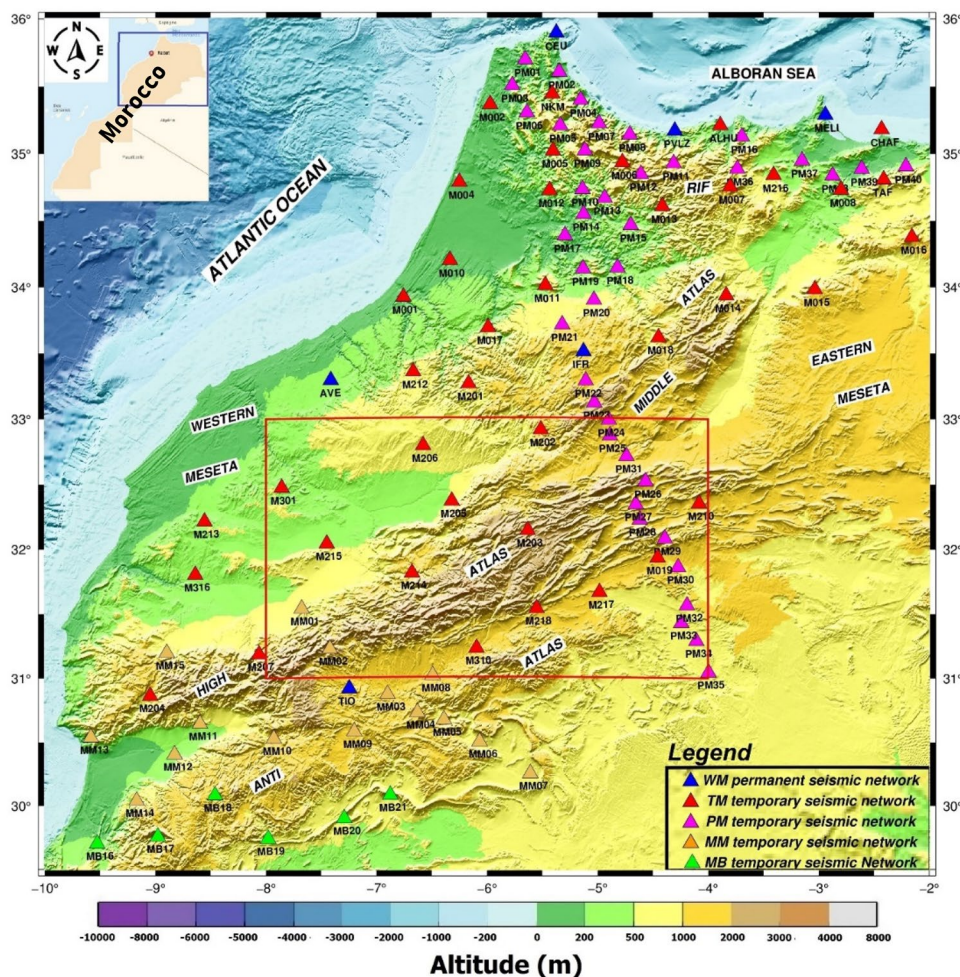
temporary station arrays (TM, MM, MB) are homogeneous and consist of Trillium 120P and Trillium 240P broadband sensors coupled with Taurus dataloggers. In the PM temporary seismic array, the equipment consists of Guralp CMG-3T and STS2 broadband sensors coupled with Quanterra Q330 dataloggers. All stations of both permanent and temporary arrays were continuously recording data samples of 100 sps.

By enhancing the permanent seismological network by deploying temporary seismic arrays, we were able to detect and record several hundreds of seismic events between the time period from 2008 to 2014. In this period, we constructed a seismic catalog which comprises seismic events with very-low to high magnitude, which cannot be possible with the poor coverage of the permanent broadband stations within the entire seismogenic areas of the country. Fifteen (15) moderate local earthquakes occurred in the area of interest, were selected from the established seismic catalog according to their magnitude level, for carrying out a seismotectonic study beneath the HMAJ area.

Methodology and data processing

First location of 15 selected earthquakes was carried out with the help of Hypocenter subroutine in Seisan software (Lienert and Havskov 1995) using the observed P-wave travel-times and the 1D layered P-wave velocity model (Table 1; Fig. 5). This latter is initially used by IGN (Instituto Geographico Nacional) and commonly used for earthquake location in many seismological studies in northern Morocco (Boulanouar et al. 2018). It was also used as a

Table 1 Initial 1D P-wave velocity model

Layer N°	Depth	Thickness	Vp	Vp/Vs
1	0-11	11	6.1	1.74
2	11-24	13	6.4	
3	24-31	7	6.9	
4	31–100	69	8.0	
5	100	–	8.2	

Fig. 5 Initial 1D velocity model (blue color and model (used by IGN).
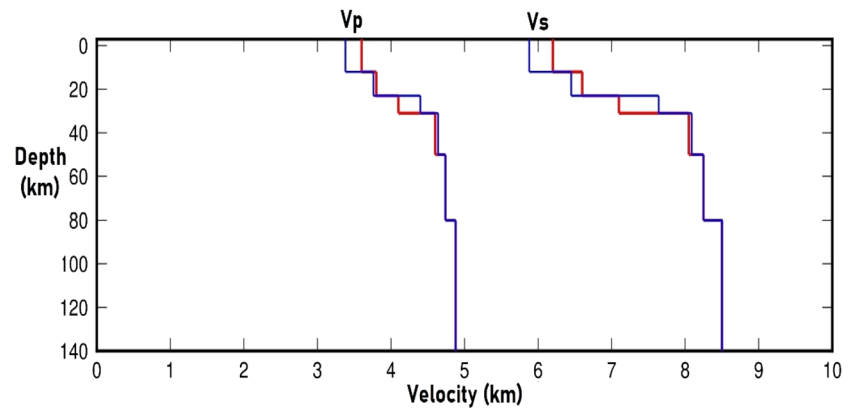
reference velocity model for seismic tomography in the collision boundary of Betics and Rif Cordilleras. A manual picking with suitable accuracy of the first P- and S-wave absolute arrival-time onsets was made on the three component seismograms for a good earthquake location. The 1D layered S-wave velocity model was retrieved by the velocity ratio:

$$V_P = 1.74^* V_S \tag{1}$$

where V_P and V_S are the P- and S-wave velocities, respectively.

To better constrain the hypocentral determinations, we calculated the minimum 1D P-wave velocity model (Fig. 5) using the joint inversion of 1D layered velocity model (used by IGN), station corrections and hypocentre locations. This inversion method is developed under **Velest** code which is based on the approach of Kissling et al. (1995). The seismic events, previously located using the IGN 1D velocity model, are carefully relocated with the minimum 1D velocity model determined in this study. The local magnitude was determined by the average of the calculated magnitude for each station using the vertical component of the seismogram.

Minimum 1D velocity model (red color).

In order to retrieve the focal mechanism solutions of the selected seismic events, we read the first motion polarities from the first impulsive P-wave onset on the vertical component of digital seismograms that were recorded at least in nine BB seismic stations. The magnitude size range of the selected moderate earthquakes and the good coverage of broadband stations enabled recording a high-level signal-to-noise ratio with clear P-wave first motion polarity reading for almost all seismic events. We then made a filter on the polarities based on the P-wave assigned weights by keeping only polarities for P-wave first motion with weights 0 and 1. With these criterions, we rejected seismic events recordings at far stations that present errors in first-motion observations. These errors may occur because of seismic station polarity reversal or incorrect P-wave arrival onsets due to low signal-to-noise ratio. We then estimated the focal mechanism parameters using FocMec program (Snoke et al. 1984), which reads in the Hypocenter output (Nordic S-file format) and computes double-couple fault plane solutions from P-wave first motion data using a grid search method (Snoke et al. 1984). The program performs an efficient systematic search of the focal beach-ball feature and reports acceptable solutions based on selection criteria for the number of polarity uncertainties. The selection criteria for both polarities and angles allow correction or weightings for near-nodal solutions.

Inversion of earthquake focal mechanisms is the widely used method for driving stress fields at seismogenic depths, by determining the best fit principal stress orientation (Gephart and Forsyth 1984; Michael 1984, 1987; Vavryčuk 2014). This method is capable of solving for the orientations of three principal stress directions and the stress ratio parameter, denoted R, which is ranging from 0 to 1:

$$R = (\sigma 2 - \sigma 3)/(\sigma 1 - \sigma 3) \tag{2}$$

where σ1, σ2, and σ3 indicate most compressive, intermediate and minimum compressive principal stresses, respectively.

To evaluate the stress parameters, we used an iterative stress inversion approach, which is implemented in the Matlab StressInverse code (Vavryčuk 2014), based on the Micheal's method (Michael 1987) and modified by Vavryčuk (Vavryčuk 2014). In this approach, the optimum stress tensor and fault plane parameters are estimated by the iterative joint inversion for stress and fault orientations from focal mechanisms. In fact, the values of four estimated stress parameters are used to evaluate the instability coefficient of nodal planes for all inverted focal mechanisms. The instability coefficient quantifies how close a fault is to an optimal direction (Vavryčuk 2011). Hence, the fault plane orientation determined in the first iteration is then used in the second iteration by performing the same procedure, which

is based on Michael's method. The procedure is reiterated until the stress reaches the optimum values (Vavryčuk 2014).

Results and discussion

Spatial distribution of the obtained hypocentre relocation and focal mechanism solutions of 15 moderate earthquakes, in relation with the tectonic structures are presented and discussed in this section. In order to well correlate the proposed seismotectonic model with previous neotectonic, seismotectonic, and geodetic models, we divided the 15 seismic events in 4 clusters of events according to their corresponding focal mechanisms and to the space-distance between the events. The state of stress in the region of interest is also discussed, based on the results of stress tensor inversion obtained, in the light of the local tectonic evolution and the regional geodynamic processes.

Relocated earthquakes and its relationship to tectonics and seismicity pattern

The obtained hypocenter relocation of the selected local earthquakes and listed in Table 2, exhibit improved horizontal determination by adding the temporary broadband stations to the permanent ones, and using the computed minimum 1D P-wave velocity model (Fig. 5). We observe a slight change in the hypocenter's location of the seismic events. The seismic events fell in the $3.0 < ML < 5.3$ magnitude

range and their depth focus was in 0–20 km range. The overall distribution of the relocated events maintains its spatial relationship to active tectonic structures in and around the HMAJ area. Moreover, the pattern of most earthquake hypocenter distribution is almost parallel to the NAF faulting system and points out the tectonic complexity which is possibly controlled by the shortening process beneath the region. In addition, three possible alignments (A1, A2 and A3) can be formed by spatial distribution of the seismic events:

- (**A1**): Group of seismic events occurs along NNE–SSW- to NE–SW-oriented zones in northern part of HMAJ area, and in correspondence with the reverse-faulting system bordering the northern part of central High Atlas (Fig. 6), enhancing non-negligible seismic activity of these tectonic structures. The horizontal distribution of these events reveals a trend along the northern boundary fault system (North Atlas Faults) and provides evidence of continuing of pre-existing fault reactivation.
- (**A2**): Another group of events appears to be crossing the area of interest with NE–SW direction (Fig. 6). The trend of this event group is almost sub-perpendicular to the compression axis of available focal mechanisms in the area and is in good accordance with the seismicity pattern beneath this part of the Atlas chain.
- (**A3**): Third group of seismic event epicenters are generally distributed in an NNW–SSE direction. According to its spatial distribution of epicenters, which is consistent with this alignment (Fig. 6). Moreover, this latter is

Table 2 Earthquake location and focal mechanism solutions of the selected earthquakes in and around the HMAJ area, and their corresponding pressure(P) and tension (T) axes are defined by their plunge and trend angles

ID	Date	O.T.	Lat. [°]	Lon. [°]	DF	M_L	Fault plane parameters					
							Strike° Φ	Dip° δ	Rake° λ	Pressure P° Az ; Pl	Tension T° Az ; Pl	Nodal B° Az ; Pl
1	2009-07-06	12:00:27 PM	31.92	–5.97	10.0	3.60	314	64	-134	174.0 ; 50.1	73.8 ; 8.5	336.9 ; 38.6
2	2010-08-05	06:54:15 PM	32.16	-5.75	11.0	4.30	235	65	75	336.1 ; 18.7	117.5 ; 66.6	241.5 ; 13.6
3	2010-08-05	06:54:14 PM	32.36	-6.07	11.0	4.30	245	60	60	356.1 ; 10.2	105.9 ; 62.1	261.1 ; 25.7
4	2011-05-01	04:50:34 AM	32.56	–4.91	12.0	3.30	225	50	50	162.1 ; 2.3	68.1 ; 60.4	253.3 ; 29.5
5	2011-02-14	06:02:56 AM	31.95	–5.78	12.0	4.40	126	85	-170	350.9 ; 10.6	260.2 ; 3.5	152.3 ; 78.8
6	2011-12-26	04:33:56 AM	31.33	–7.29	16.0	3.58	340	70	-142	202.8 ; 40.6	104.4 ; 9.6	3.6 ; 47.8
7	2011-12-26	04:33:54 AM	31.34	–7.32	13.0	3.40	225	55	0	185.7 ; 23.9	84.3 ; 23.9	315.0 ; 55.0
8	2013-04-27	09:21:26 AM	32.34	–5.53	8.4	4.60	35	52	90	305.0 ; 13.0	125.0 ; 77.0	35.0 ; 0.0
9	2013-05-27	08:07:10 PM	32.24	–6.26	9.1	4.50	237	60	84	331.4 ; 14.8	131.2 ; 74.3	240.0 ; 5.2
10	2013-05-31	08:46:26 AM	32.39	–5.39	7.6	5.20	32	63	90	122.0 ; 18.0	302.0 ; 72.0	32.0 ; 0.0
11	2013-05-31	02:46:03 PM	32.43	–5.38	5.2	4.90	70	15	90	340.0 ; 30.0	160.0 ; 60.0	70.0 ; 0.0
12	2013-06-25	01:09:55 PM	32.41	–5.34	13.7	4.50	28	58	90	118.0 ; 13.0	298.0 ; 77.0	28.0 ; 0.0
13	2014-03-12	12:27:09 PM	32.45	–6.20	5.2	4.10	30	50	90	120.0 ; 5.0	300.0 ; 85.0	30.0 ; 0.0
14	2014-05-12	03:53:21 AM	32.24	–6.18	5.5	5.00	45	50	90	135.0 ; 5.0	315.0 ; 85.0	45.0 ; 0.0
15	2014-05-19	12:09:28 PM	32.38	–5.60	6.4	4.30	30	55	90	120.0 ; 10.0	300.0 ; 80.0	30.0 ; 0.0

The second nodal plane has been described by the B-axes (trend, plunge)

Fig. 6 Spatial distribution of 15 relocated earthquakes; the cyan stars indicate the epicenters of the relocated earthquakes. A1, A2 and A3 blue shot lines indicate possible alignments of these seismic event epicenters. Triangles are seismic stations in and around the area of study
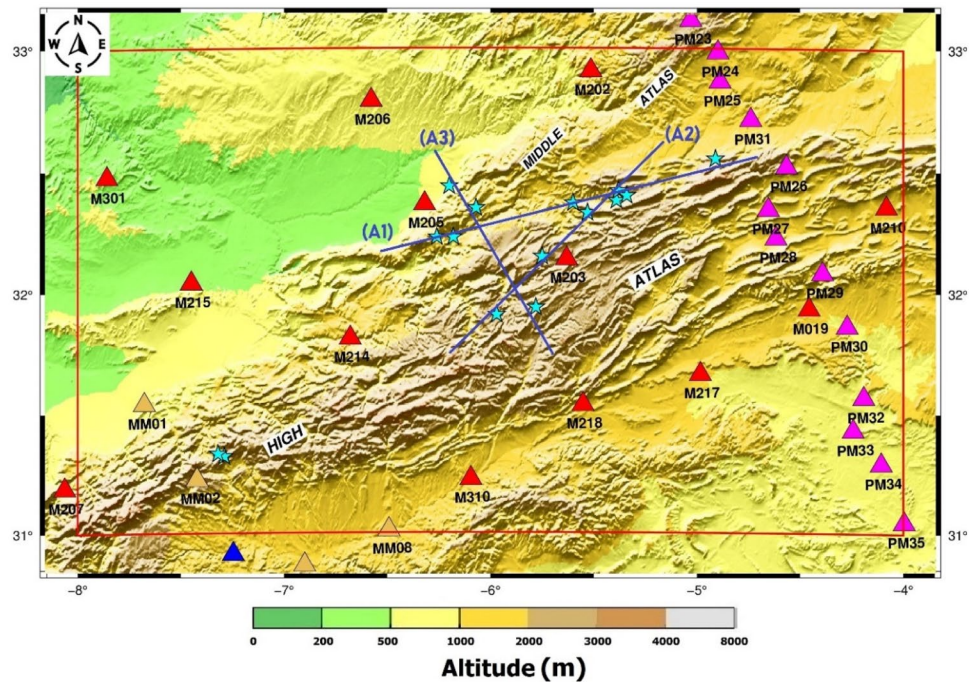
coincident with the junction zone between the Middle Atlas and the High Atlas, crossing the North and South Atlas fault systems and the internal fault segments in the Imilchil area (around M203 station) are splitting by this alignment (Onana et al. 2011).

Focal mechanisms solutions

New focal mechanisms were determined for the fifteen (15) local and moderate crustal seismic events that occurred in the area of HMAJ and recorded from 2007 to 2014. The fault plane solutions of these 15 seismic events are listed in Table 2 and represented by their strike, dip and rake fault plane solution parameters. The trend and the plunge angles of the pressure (P-axis) and the tension (T-axis) axes, respectively, are also calculated by the grid search method. The similarity and diversity of the obtained earthquake focal mechanisms are displayed in ternary diagram (Frohlich 1992; Hallo 2018) for an easy classification by type of all faults (Fig. 7). A global view of the focal mechanisms obtained in this study, based on the fault plane solutions, reveals the presence of variability of mechanisms, but the compressive faulting mechanism is predominant beneath the region of interest (Figs. 7 and 8).

The first nodal plane's parameters (strike, slip, rake) are summarized in Table 2 and represented by the stereographic representation (with trends and plunges of P- and T-axes) in Figs. 8 and 9, while the second nodal plane being described by the B-axes (trend, plunge). Thus, each focal mechanism can be represented by their tectonic axes P, T
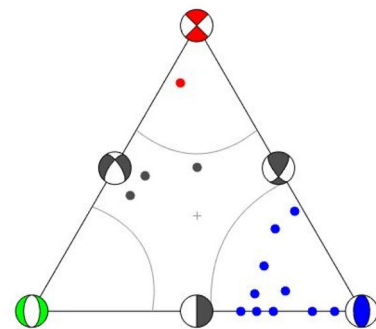

Fig. 7 Ternary diagram representing the distribution of faulting mechanism types. Curved lines are boundaries with T-, B- and P-axes of 40°, 30° and 30° from vertical, respectively (Frohlich 2001)

and B (Table 2). Based on the trend and plunge angles of P-axes and T-axes of 15 fault plane solutions (Table 2), the average trend with their corresponding systematic errors of the pressure (P) axes and tension (T) axes, related to these focal mechanisms, is 223.94°±95.6° and 17.68°±13.02°, respectively, while the average plunge with their corresponding systematic errors of the pressure (P) axes and tension (T) axes, associated to 15 earthquake focal mechanisms, is 183.02°±95.22° and 56.32°±28.41°, respectively.

According to the focal mechanism type, eleven (11) seismic events show a reverse (thrust) faulting mechanism, four of which have a strike-slip component. Their corresponding P-axes are distributed along the NW–SE to NNW–SSE trends, with slightly variable plunges (Fig. 9).
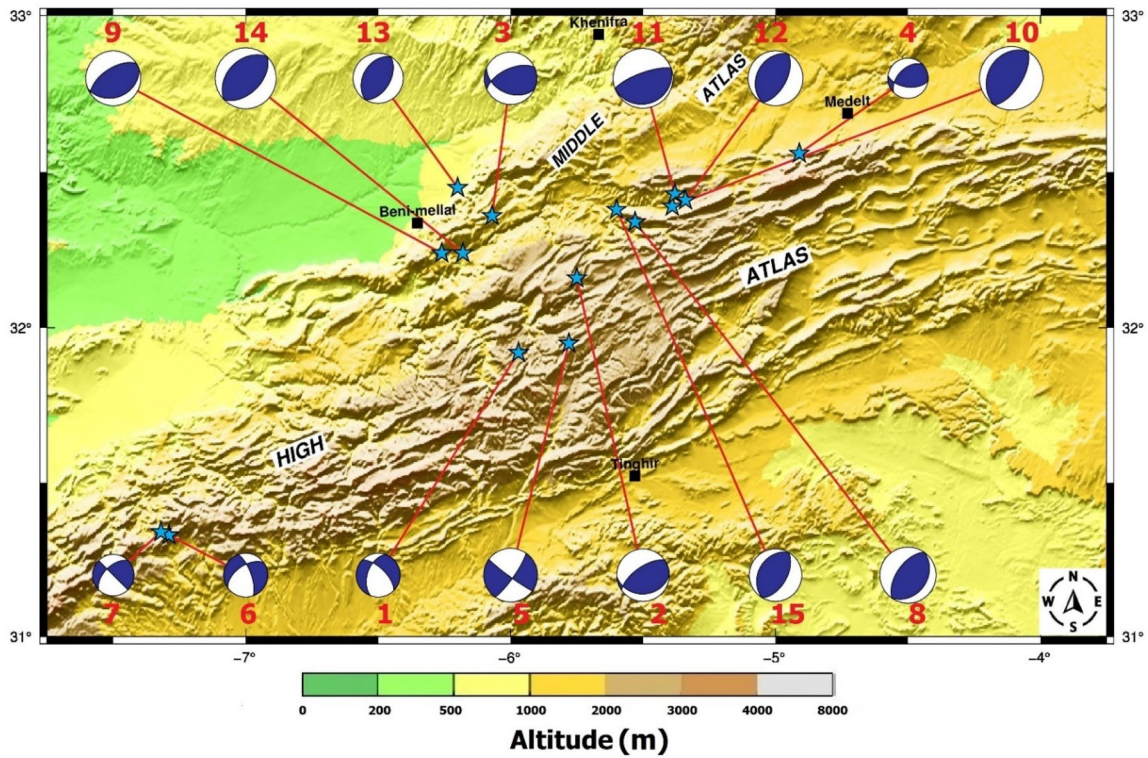
Fig. 8 Seismotectonic model beneath the HMAJ area: earthquake focal mechanisms determined in the present study. The size of beach balls is proportional to the magnitude, which ranges between 3.3 and 5.2. The cyan stars represent the epicenters of selected earthquakes in this study. The blue shaded area in the stereographic focal mechanism represents compressional quadrants and the white open area dilatational quadrants
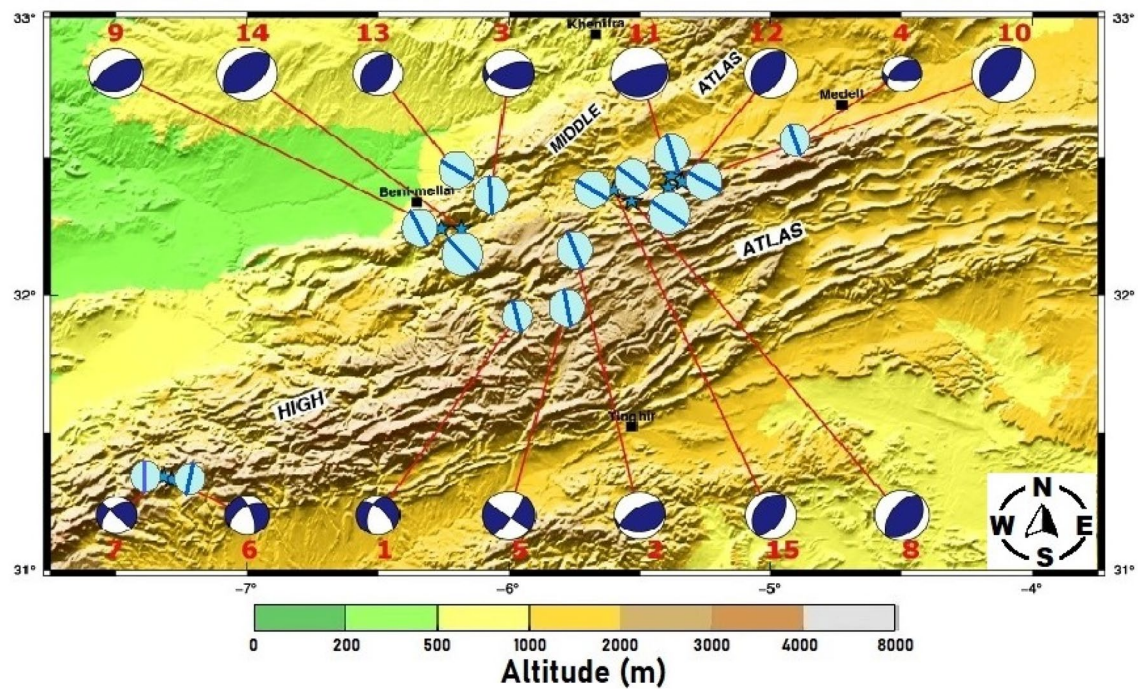
Fig. 9 Seismotectonic model beneath the HMAJ area; orientation of P (Pressure)-axes of focal mechanism solutions are indicated by thick blue bars inside cyan circles coincide with the epicenters of analyzed seismic events

One of the analyzed focal mechanisms corresponds to strike-slip faulting with a normal component, with the P-axis trending along the NNE–SSW. In addition, three odd mechanisms with strike-slip components are also observed in the analyzed events, in which the corresponding P-axes have a general orientation along the NNW–SSE to NS trends. Previous focal mechanisms data of moderate earthquakes occurred in the region of interest and reported by different agencies (Harvard CMT, INGV, IGN, GFZ) and by several seismotectonic studies (Medina et al. 1992 ; Medina 2008 ; Bensaid et al. 2011 ; Martin et al. 2015) reveal almost the same compressive regime that governs the local and regional tectonic deformation processes within the study area.

In order to correlate the obtained focal mechanism solutions with the findings in previous seismotectonic and geodynamic studies carried out beneath the area of study, we split the 15 seismic events, ordered from 1 to 15 (Table 2), into four clusters; C1 (events IDs: 4, 8, 10, 11, 12, 15), C2 (events IDs: 1, 9, 13 and 14), C3 (events IDs: 1, 2 and 5), and C4 (events IDs: 6 and 7), according to their geographical distribution within Z1, Z2, Z3 and Z4 zones, and to the space-distance between the events (Fig. 10):

- **Cluster C1**:

First cluster of six seismic events is located within zone Z1 (Fig. 10) at the northern boundary of the HMAJ. Four events (with IDs; 8, 10, 12 and 15) among this cluster exhibit almost identical pure reverse focal mechanisms that could be related with the fault sectors of north Atlas fault (NAF) and their secondary faults network. The orientation of their P-axes reveal a NW–SE trending (Fig. 9) which almost coincides with the orientation of the compressive convergence between Nubia and Eurasia plates and is consistent with GPS velocities (Koulali el al. 2011). One seismic event (with IDs: 4) shows the reverse-faulting mechanisms with strike-slip component, with a compressional P-axis oriented to NNW–SSE trending. The later event in this cluster (with ID; 11) presents a reverse faulting which is characterized by a large P-axis plunge along the NNW–SSE orientation. Thus, the compressive faulting retrieved from the focal mechanism analysis of this cluster displays a general compression NE–SW to NNS–SSW orientation which are nearly perpendicular to the average fault plane orientation of the active tectonics fault planes, as shown by RD1 rose diagram (Fig. 10), beneath Z1 zone including this cluster of seismic events. Further east to Z1 zone, one moderate earthquake happened in 2019 and largely felt in the area of Midelt and neighboring provinces (Medina et al. 2021) exhibit a strike-slip faulting (from CGMT, INGV, GFZ seismological agencies), with a horizontal P-axis oriented in NNE–SSW trend
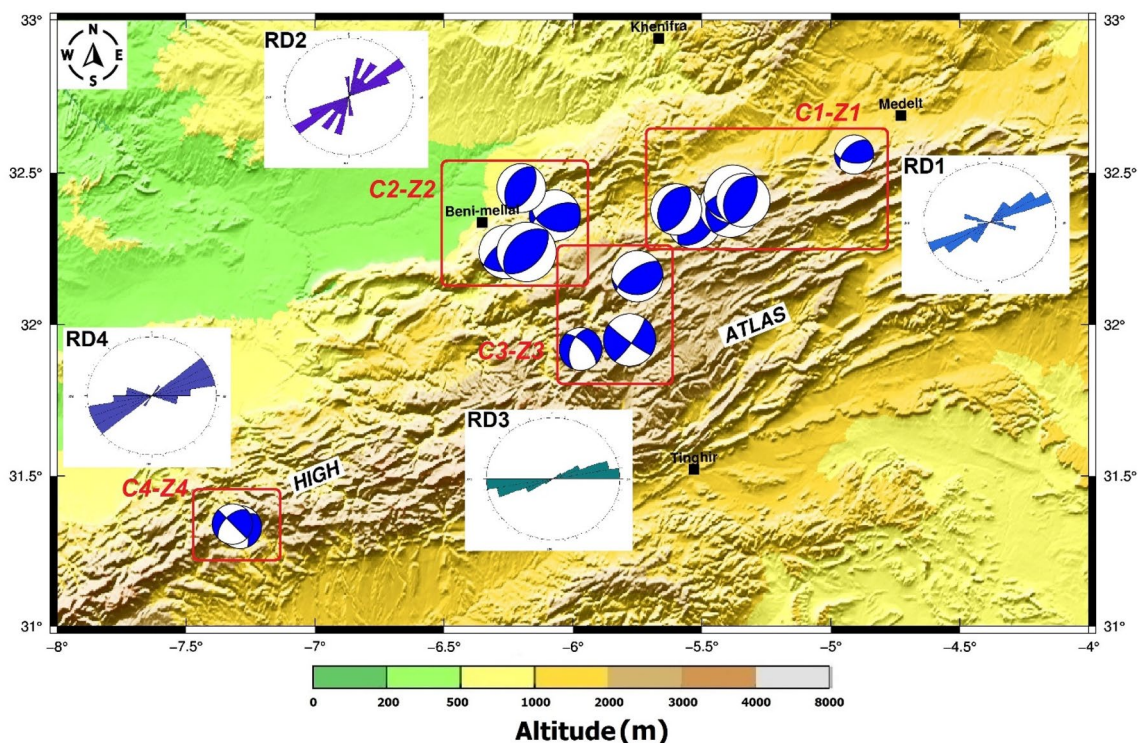
Fig. 10 Map of seismotectonic model showing the focal mechanisms of the seismic events. C1, C2, C3 and C4 are, respectively, the seismic event clusters within Z1, Z2, Z3 and Z4 zones. RD1, RD2, RD3 and RD4 are rose diagrams of active tectonic faults beneath each zone

(Fig. 11), is in a good agreement with dominant faulting regime beneath Z1 zone.

- **Cluster C2**:

Further west to the cluster C1, the second cluster, C2, which is composed of 4 seismic events (with IDs; 3, 9, 13, 14), is also located close to the northern boundary of the area of study and around to the Beni-Mellal province (Fig. 10). The fault plane solutions of three events (with IDs; 9, 13 and 14) show a compressive faulting mechanisms with a global horizontal P-axes trending to NE–SW direction as for seismic events of cluster C1, except one event (with Id; 3), which exhibit the same faulting mechanism with strike-slip component and their P-axis trends to N–S direction (Fig. 9). These compressive faulting orientations are steeply related to the motion direction of both lithospheric plates, Nubia and Eurasia, and coherent with GPS field patterns (Koulali et al. 2011). Moreover, the compressive orientation of C2 mechanisms is almost perpendicular to the general

orientation of active tectonic fault planes, as displayed by the RD2 rose diagram, beneath the Z2 zone (Fig. 10). Hence, the presence of moderate seismic events observed in Z2 zone with those in Z1 zone show that the northern boundary of HMAJ area is exposed to an active tectonics with dominant reverse-faulting regime, enhancing the assumption of the slight crustal shortening at boundaries of this region of the High Atlas system (Frizon de Lamotte et al. 1985 ; Gomez et al. 1996 ; Teixell et al. 2003).

- **Cluster C3**:

The three seismic events (with IDs; 1, 2 and 5) of this cluster C3 are located in the middle of HMAJ, far from the boundaries of central High Atlas. All mechanisms corresponding to these events reveal a heterogeneous faulting pattern which explains the change of orientation stress field beneath the Z3 zone (Fig. 10). However, fault plane solutions show the presence of reverse, strike-slip and odd faulting that explain a local change of tectonic deformation
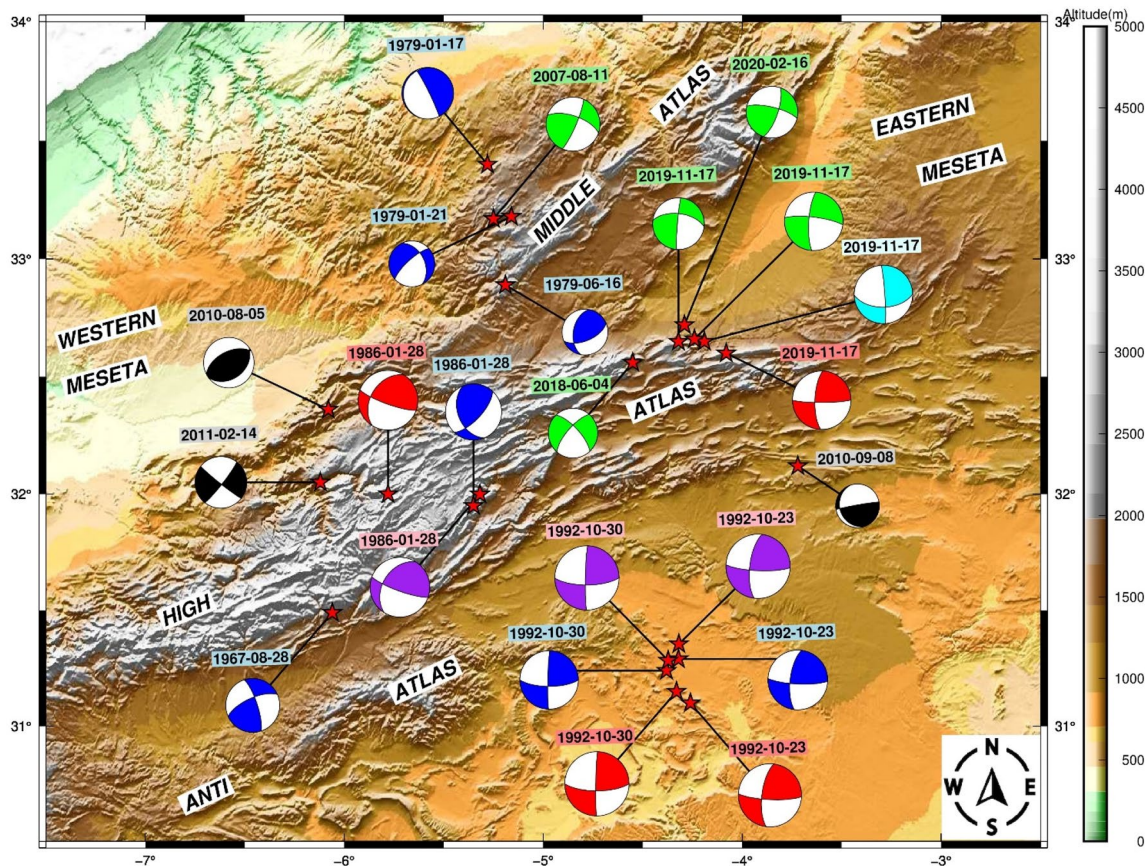
Fig. 11 Compilation of available focal mechanisms (Medina 2008, 2010; Bensaid et al. 2011; Martin et al. 2015) and seismological agencies INGV, Harvard (GCMT), USGS, GFZ), determined in and around the Middle-High Atlas junction, plotted on a topographic map of Morocco. Background map is a courtesy of National Centers of Environmental Information, USA. The red stars indicate the earthquake epicenters of corresponding stereographic representation of focal mechanisms

directions when we pass from the boundaries to the interior of the central High Atlas, and consequently we could observe a mixture and variability of focal mechanism types. Two solutions from available focal mechanisms, within Z3 zone, determined in previous study using moment tensor inversion (Martin et al. 2015), present reverse and strike-slip focal mechanisms with a compressive trending to NNE–SSW and N–S direction (Fig. 9), respectively. Indeed, the reverse-faulting mechanism corresponding to the event of 2008 (2008-08-06) (Fig. 11) and their P-axis orientation is in agreement with the same one (with ID; 2) analyzed in this study (Fig. 8). The second event occurred in 2011 (2011-02-04)) (Fig. 11) exhibits a strike-slip focal mechanism with corresponding P- and T-axes, which are very similar to those obtained for the seismic event (with ID; 5) analyzed in this work.

- **Cluster C4**:

Further southwest to C3 cluster, focal mechanisms corresponding to two events (with IDs; 6 and 7) (Fig. 8) of C4 cluster in Z4 zone, display odd faulting with horizontal P-axes trending to NNE–SSW and N–S directions (Fig. 9). respectively. The perpendicular direction to the average active fault plane orientation within Z4 zone, from neotectonic data as shown in RD4 rose diagram (Fig. 10), is oblique to the fault trending direction of P-axes of two seismic events. Although the epicenters of these two earthquakes of the C4 group are located far from the epicenters of other groups of earthquakes, we observe then the pressure axes relating to their focal mechanisms have almost the same global orientation as other pressure axes of the focal mechanisms of seismic events constituting the other clusters (C1, C2 and C3). Analysis of geodetic GPS data shows that the central high Atlas (including HMAJ area) is slowly deforming and the vector orientations confirm the effects of the occurrence of seismicity along the general faulting trends NE–SW to ENE–WSW (Koulali et al. 2011).

Comparison with previous available focal mechanisms beneath the Atlas chain

The earthquake focal mechanisms determined in atlas chain were carried out in numerous seismotectonic studies (Medina and Cherkaoui 1991, 1992 and 2021; Medina 2008; Medina et al. 2011; Martin et al. 2015) and many seismological agencies as shown in Fig. 11:

- In the central High Atlas, the focal mechanism solutions of moderate seismic events were mainly determined for seismic events of 28/08/1967 and 28/01/1986. All solutions correspond to reverse faulting with strike-slip component. The trends of the P-axes are NW–SE in

both cases. The solution of the 14/02/2011 event correspond to pure strike-slip faulting with NNW–SSE-trending P-axis.

- Towards the east, three focal mechanism solutions of the event of 17/11/2019 were determined by agencies. All describe a strike-slip faulting with average P-axes trending to NW–SW direction. Another event of 04/06/2018 corresponding to strike-slip occurred close to the latter one, with P-axis trends to N–S.

- To the north of the central high Atlas, there are only four mechanisms determined for the (17/01/1979) and 16/06/1979 earthquakes. The three solutions of the first one correspond to normal faulting with WSW–ENE-trending P-axes, while the second solution describes reverse faulting with NW–SE-trending P-axis (Medina 2008). Solution of the event of 11/08/2007 shows a strike-slip faulting with a large reverse component. The P-axis of the later event trends to the NNW–SSE direction.

- Further south, in the Anti-Atlas, the mechanism of the Rissani earthquake of 23/10/1992 and 30/10/1992 shows a strike-slip faulting with P-axes oriented to NW–SW.

- On the basis of the compiled available focal mechanisms from seismotectonic studies and seismological agencies (Fig. 11), the trend of P-axes NE–SW to NNW–SSE corresponding to the dominant compressional faulting regime is currently controlling the area of study and agrees well with that determined for most analyzed focal mechanisms in this study (Fig. 9). Despite few events characterized by strike-slip or odd faulting regime, their corresponding P-axes are oriented to NW–SE, NNW–SSE and N–S trending.

Gathered focal mechanism solutions for earthquakes occurred in and around the HMAJ area from seismotectonic studies (Medina et al. 2011; Medina 2008; Medina et al. 1991; Martin et al. 2015) and from agencies (INGV, GCMT, GFZ), revealed a spatial variability of the faulting mechanisms and orientation of its pressure axes. Analysis of the focal mechanisms combined from those determined in this study and those available previously indicates a reorientation of the compression faulting regime between the northern boundary of central High Atlas, particularly in HMJA area, into eastern High Atlas from compressive to a strike-slip movement (Fig. 11). The NNE–SSW average compressive orientation revealed by the analysis of focal mechanisms is generally consistent with the recent geodetic GPS velocities field feature (Koulali et al. 2011). Moreover, the compressional reverse faulting and its orientations beneath the central High Atlas are currently accommodating the Atlas system tectonics and confirming the motion of the Nubia plate towards the Iberian Peninsula.

In comparison with adjacent seismogenic areas, further north to Atlas belt, several seismotectonics studies were carried out beneath the tectonic structure of Rif domain to derive the tectonic evolution and the faulting regime. Most results show a similar pressure axes pattern (NNE–SSW) derived from moment tensor and first motion focal mechanism, but with predominant strike-slip faulting mechanism in the eastern Rif and beneath the famous seismogenic area of Al Hoceima (Martin et al. 2015; Stich et al. 2010; Buforn et al. 1995; Medina 2008). Moreover, in this later area, three famous events with magnitude exhibit similar strike-slip focal mechanism solutions with NNE–SSW-trending left-lateral faulting for the 1994 and 2016 events and NW–SE-trending right-lateral faulting for the 2004 event. Similar pattern(NW–SE) is also observed with compressive stresses in the region Alboran Sea (Kariche et al. 2018).

Stress field analysis

It is admitted in seismotectonic studies that moderate-to-large magnitude earthquakes are related to regional stress fields, while low magnitude ones are related to local stress or block adjustments. Theoretically, the pressure (P) and tension (T) axes defining a focal mechanism solution, located 45° to the two nodal planes, do not perforce reflect the stress and strain axes (Mckenzie 1969) which occurs at an angle closer to 30° to the primary principal stress axis according to the Mohr-Coulomb failure criterion. In fact, there are approximately 15° discrepancies between the P- and T-axes and the axis of principal stress. Thus, inversion of stress tensor is one adequate procedure of reducing this uncertainty, by considering clusters of focal mechanisms assumed to derive from a common stress tensor. In order to estimate the stress tensor and analyze the state of the stress field beneath the region of study, we grouped all focal mechanism solutions (strike, dip and rake angles) and then inverted them using the method inversion of Michael (1987) and modified by Vavryčuk (2014). Stress field results

are summarized in Fig. 12B and show that the stress tensor reflects the clear orientations shown by the analyzed focal mechanisms.

Orientation of stress fields in HMJA area inferred from stress tensor inversion exhibit mostly similar direction (NNE–SSW trending) as those shown by general pressure (P-axes) orientations (Figs. 9 and 11B) deduced from grid search focal mechanism method. In fact, the stress field of reverse-faulting style is dominant in the HMAJ area. In addition, their principal stress directions show that the axis of σ1 has the trend of 178.0° and dipping southward of 2.0° and an axis of σ2 has the trend of 268.0° and the dipping westward of 3.0°, indicating that both of σ1 and σ2 axes are sub-horizontal. The third stress axis, σ3, has the trend of 46.0° and the plunge of 87.0°, and tends to be sub-vertical. The stress shape ratio, R, is equal to 0.61 in the whole area (Fig. 12-C).

> stereographic projection of percent confidence regions of principal stress axes Pressure–Tension axes (red–blue, respectively) on the focal sphere are also shown. **C** Histogram of shape ratio.

Determination of the stress field state was possible due to the homogeneous character of the mechanism cluster due to the occurrence of almost one possible tectonic regime reflected by predominant compression stress in the region of interest. The distribution of the stress field is consistent with the faulting style observed for major faults. Indeed, predominant reverse-faulting style with maximum compressional stress trending to NNW–SSW is now characterizing HMJA area (Fig. 12). According to previous geotectonic studies, the orientation of the maximum horizontal stress rotated from NNE–SSW to NNW–SSE from the early Paleocene to the Neogene (Fekkak et al. 2018). Movement along these structures is consistent with a compressive stress component σ1 oriented NNW–SSE (Ait Brahim et al. 2002). This ultimate tectonic process is responsible for the loud uplift of the Atlas belt and the folding of its foreland, and consequently enhancing the tectonic shortening process due to the compression
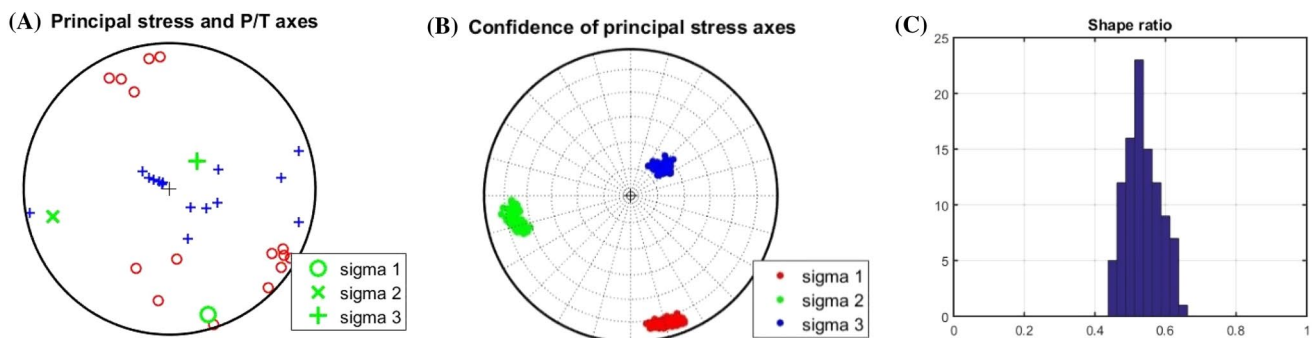
Fig. 12 **A** Distribution of P (pressure)–T (tension) (red–blue, respectively) axes and principal stress axes (green), **B** the

during the Eocene and Pliocene-Quaternary along the Atlas Formation (Teixell et al. 2003). Such investigation on seismic anisotropy components beneath the tectonic structures could help to infer characteristics and more information of the stress field beneath the study area.

Conclusion

The good coverage of broadband stations of the implemented seismic arrays in and around the HMJA area and the computed minimum 1D velocity model have systematically improved the relocation of the selected seismic events. By analyzing these events, we proposed a seismotectonic model, based on results of reliable focal mechanisms and stress tensor analysis. Solutions suggested from the calculated mechanisms enabled to observe a dominant reverse-faulting system beneath the northern part of the area of interest. In addition, their fault planes almost coincide with tectonic fault sectors composing the major Northern Atlas Fault (NAF). Moreover, the pressure (P) axis of all analyzed seismic events exhibit a NW–SE to NNE–SSW sub-horizontal direction for most faulting mechanisms. The heterogeneous faulting pattern observed for few earthquakes, located far-off the boundaries of the HMAJ area, may indicate varying the conditions of local stresses. Thus, by performing a stress tensor inversion to the obtained foal mechanism solutions, we have inferred the state of the tectonic stress field that governs the HMAJ area. Results of the principal stress tensor parameters reveal that the attitudes (trend/plunge) of the principal stress axes are $\sigma 2 = 178.0°/2.0°$, $\sigma 2 = 268.0°/3.0°$ and $\sigma 3 = 46.0°/87.0°$, suggesting that the region of study is currently subjected to a maximum sub-horizontal compressional stress along NNW–SSE direction. Consequently, these results show that the seismotectonic model derived from focal mechanisms with mainly reverse-faulting style and maximum stress orientation fairly well agree with: (1) available earthquake focal mechanisms in the Atlas area, determined in previous studies and mentioned in Agencies catalogs, (2) the regional geotectonic and geodynamic models that states the relative motion trending NW–SE of Nubian plate towards Eurasia plate, (3) the recent geodetic model derived from GPS velocity field orientation (Koulali et al. 2011), and (4) NW–SE compressional stress pattern during the Plio-Quaternary as indicated by the neotectonic models.

Indeed, the seismotectonic model developed in this study by the combination of the analysis of seismological and geotectonic data, allowed to establish links between seismic activity and current tectonic deformation mechanisms and to pinpoint potential seismic sources within the HMAJ area. Furthermore, it can then be used to conduct a reliable seismic hazard assessment beneath the area of study. However, more efforts should be made by collecting more instrumental seismicity data, as well as gathering more geotectonic information to carry out a more complete seismotectonic model for this seismogenic region.

Declarations

Conflict of interest The authors declare that there is no conflict of interest.

References

Abdulnaby W, Al-Mohmed R, Mahdi M (2016) Seismicity and recent stress regime of Diyala City, Iraq–Iran border. Model Earth Syst Environ 2:142. https://doi.org/10.1007/s40808-016-0201-z

Ait Brahim L, Chotin P (1984) Mise en évidence d'un changement de direction de compression dans l'avant pays rifain (Maroc) au cours du Tertiaire et du Quatemaire. Buil Soc go/ Fr 4:681–689

Ait Brahim L, Chotin P, Hinaj S, Abdelouafi A, El Adraoui A, Nakcha C, Dhont D, Charroud M, Alaoui FS, Amrhar A, Bouaza A, Tabyaoui H, Chaouni A (2002) Paleostress evolution in the Moroccan African marginfrom Triassic to Present. Tectonophysics 357:187–205

Angelier J (1984) Tectonic analysis of fault slip data sets. J Geophys Res Solid Earth 89(B7):5835–5848

Ayarza P, Carbonell R, Teixell A, Palomeras I, Martí D, Kchikach A, Harnafi M, Levander A, Gallart J, Arboleya ML, Alcalde J (2014) Crustal thickness and velocity structure across the moroccan Atlas from long offset wide-angle reflection seismic data: the SIMA experiment. Geochem Geophys Geosyst 15(5):1698–1717

Bensaid I, Buforn E, Cherkaoui TE, Medina F, Hahou Y (2011) New fault-plane solutions of moroccan earthquakes for the 2005–2008 period. Bull Inst Sci sect Sci Terre 33:47–52

Bernini M, Boccaletti M, Moratti G, Papani G (2000) Structural development of the Taza-Guercif Basin as a constraint for the Middle Atlas Shear Zone tectonic evolution. Mar Pet Geol 17(3):391–408

Bezada MJ, Humphreys ED, Davila JM, Carbonell R, Harnafi M, Palomeras I, Levander A (2014) Piecewise delamination of moroccan lithosphere from beneath the Atlas Mountains. Geochem Geophys Geosyst 15:975–985. doi:https://doi.org/10.1002/2013GC005059

Boulanouar A, El Moudnib L, Padhy S, Harnafi M, Villasenor A, Gallart J, Pazos A, Rahmouni A, Boukalouch M, Sebbani J (2018) Estimation of coda wave attenuation in Northern Morocco. Pure Appl Geophys 175:883–897

Buforn E, Sanz de Galdeano C, Udías A (1995) Seismotectonics of the Ibero-Maghrebian Region. Tectonophysics 248:247–261

Buforn E, Bezzeghoud M, Udías A, Pro C (2004) Seismic sources on the Iberia-African plate boundary and their tectonic implications. Pure appl Geophys 161(3):623–646

Cherkaoui T-E, El Hassani A (2012) Seismicity and seismic hazard in Morocco: 1901–2010. Bulletin de l'Institut Scientifique. Rabat Sect Sci de la Terre 34:45–55

Frizon De Lamotte D, Crespo-Blanc A, Saint-Bezar B, Comas M, Fernandez M, Zeyen H, Ayarza P, Robert-Charrue C, Chalouan A, Zizi M, Teixell A, Arboleya ML, Alvarez-Lobato F, Julivert M, Micard A (2004) TRANSMED-transect I (Betics, Alboran Sea, Rif, Moroccan Meseta, High Atlas, Jbel Saghro, Tindouf basin. In: W Cavazza, F Roure, W Spakman, GM Stampfli, pA Ziegler (eds) The TRANSMED Atlas: the Mediterranean region from crust to mantle. Springer, Berlin. https://hal.archives-ouvertes.fr/hal-00069189/

Dooley TP, Hudec MR (2020) Extension and inversion of salt-bearing rift systems. Solid Earth 11:1187–1204

Fekkak A, H. Ouanaimi H, Michard A, Soulaimani A, Ettachfini EM, Berrada I, El Arabi H, Lagnaoui A, Saddiqi O, (2018) Thick-skinned tectonics in a Late Cretaceous-Neogene intracontinental belt (High Atlas Mountains, Morocco): The flat-ramp fault control on basement shortening and cover folding. J Afr Earth Sci 140:169–188

Frizon de Lamotte D, Saint Bézar B, Bracène R, Mercier E (2000) The two main steps of the Atlas building and geodynamics of the western Mediterranean. Tectonics 19:740–761

Frohlich C, Apperson KD (1992) Earthquake focal mechanisms, moment tensors, and the consistency of seismic activity near plate boundaries. Tectonics 11(2):279–296

Gephart JW, Forsyth DW (1984) An improved method for determining the regional stress tensor using earthquake focal mechanism data: application to the San Fernando Earthquake sequence. J Geophys Res Solid Earth 89(11):9305–9320

Gomez F, Barazangi M, Bensaid M (1996) Active tectonism in the intracontinental Middle Atlas Mountains of Morocco: synchronous crustal shortening and extension. J Geol Soc 153(3):389–402

Hallo M, Opršal I, Asano K, Gallovič F (2019) Seismotectonics of the 2018 Northern Osaka M6.1 earthquake and its aftershocks: joint movements on strike-slip and reverse faults in inland Japan. Earth Planet Space 71:34

Havskov J, Ottemoller L (1999) SeisAn earthquake analysis software. Seismol Res Lett 70(5):532–534

Jacobshagen V (1988) The Atlas system (Morocco). Springer-Verlag, New York, pp 481–499

Kariche J, Meghraoui M, Timoulali Y, Cetin E, Toussaint R (2018) The Al Hoceima earthquake sequence of 1994, 2004 and 2016: Stress transfer and poroelasticity in the Rif and Alboran Sea region. Geophys J Int 212:42–53

Kissling E, Ellsworth WL, Eberhart-Phillips D, Kradolfer U (1994) Initial reference models in local earthquake tomography. J Geophys Res 99:19635–19646

Koulali A, Ouazar D, Tahayt A, King RW, Vernant P, Reilinger RE (2011) New GPS constraints on active deformation along the Africa–Iberia plate boundary. Earth Planet Sci Lett 308(1–2):211–217

Laville E, Piqué A (1992) Jurassic penetrative deformation and cenozoic uplift in the central high Atlas (Morocco): a tectonic model. Structural and orogenic inversions. Geol Rundsch 81:157–170

Lee H, Bezada MJ, Faccenda M (2021) Can sub-slab low-velocity anomalies be an artifact caused by anisotropy? A case study from the Alboran slab area in the western Mediterranean. Tectonophysics 229080. https://doi.org/10.1016/j.tecto.2021.229080

Lee HM, Bezada MJ, Kim YH (2022) The origin of the low-velocity anomalies beneath the rootless atlas mountains: insights gained from modeling of anisotropy developed by the travel of canary plume. JGR Solid Earth. https://doi.org/10.1029/2022JB024622

Lienert BRE, Havskov J (1995) A computer program for locating earthquakes both locally and globally. Seismol Res Lett 66(5):26–36

Makris J, Demnati A, Klussmann J (1985) Deep seismic soundings in Morocco and a crust and upper mantle model deduced from seismic and gravity data. Ann Geophys 3:369–380

Martín R, Stich D, Morales J, Mancilla F (2015) Moment tensor solutions for the Iberian-Maghreb region during the Iberarray deployment. Tectonophysics 663:261–274

Mckenzie DP (1969) The relation between Fault Plane solution for earthquakes and the directions of the principal stresses. Bull Seismol Soc Am 59:591–601

Medina F (2008) Catalogue of focal mechanisms of the moroccan earthquakes for the period 1959–2007. Doc Inst Sci Rabat 23:58

Medina F, Cherkaoui TE (1991) Focal mechanisms of the Atlas earthquakes, and their tectonic implications. Geol Rundsch 80:639–648

Medina F, Cherkaoui TE (1992) Mécanismes au foyer des séismes du Maroc et des régions voisines (1901–1986). Implications tectoniques. Eclogae Geol Helv 85:(2):433–457

Medina F, Cherkaoui TE (2021) The Midelt earthquake of November 17th 2019, and its implications on the present-day tectonics of the junction of the High and Middle Atlas (Morocco). Arab J Geosci 14:1717

Medina F, Bensaid I, Tangi A (2011) Catalogue of focal mechanisms of Moroccan earthquakesf or the period 1959–2007; analysis of parameters. Bulletin de l'Institut Scientifique Rabat section Sciences de la Terre 33:37–46

Michael AJ (1984) Determination of stress from slip data: faults and folds. J Geophys Res 89:(11):517–526

Michael AJ (1987) Use of focal mechanisms to determine stress: a control study. J Geophys Res 92:357–368

Miller MS, Allam AA, Becker TW, Di Leo JF, Wookey J (2013) Constraints on the tectonic evolution of the westernmost Mediterranean and northwestern Africa from shear wave splitting analysis. Earth Planet Sci Lett. https://doi.org/10.1016/j.epsl.2013.05.036

Missenard Y, Taki Z, Frizon de Lamotte D, Benammi M, Hafid M, Leturmy P, Sébrier M (2007) Tectonic styles in the Marrakesh High Atlas (Morocco): the role of heritage and mechanical stratigraphy. J Afr Earth Sci 48(4):247–266

Morel JL, Zouine M, Andrieux J, Faure-Muret A (2000) Déformations néogènes et quaternaires de la bordure nord haut atlasique (Maroc): Rôle du socle et conséquences structurales. J Afr Earth Sci 30:119–131

Mridekh A, Toto EA, Hafid M, El Ouataoui A (2000) Structure sismique de la plate-forme atlan-tique au large d'Agadir (Maroc sud-occidental). Comptes Rendus de l'Académie des Sciences de Paris. Sci de la Terre et des Planètes 331:387–392

Mutlu AH (2020) Seismicity, focal mechanism, and stress tensor analysis of the Simav region, western Turkey. Open Geosci. https://doi.org/10.1515/geo-2020-0010

Onana PNE, Toto EL, Zouhri L, Chaabane A, El Mouraouah A, Iben Brahim A (2011) Recent seismicity of Central High Atlas and Ouarzazate basin (Morocco). Bull Eng Geol Environ 70:633–641

Palomeras I, Thurner S, Levander A, Liu K, Villaseñor A, Carbonell R, Harnafi M (2014) Finite-frequency Rayleigh wave tomography of the western Mediterranean: mapping its lithospheric structure. Geochem Geophys Geosyst 15:140–160

Palomeras I, Villaseñor A, Thurner S, Levander A, Gallart J, Harnafi M (2017) Lithospheric structure of Iberia and Morocco using finite-frequency Rayleigh wave tomography from earthquakes and seismic ambient noise. Geochem Geophys Geosyst 18:1824–1840

Sebrier M, Siame L, Zouine EM, Winter T, Missenard Y, Leturmy P (2006) Active tectonics in the moroccan high Atlas. C R Geosci 338(1–2):65–79

Serpelloni E, Vannucci G, Pondrelli S, Argnani A, Casula G, Anzidei M, Baldi P, Gasperini P (2007) Kinematics of the Western Africa–Eurasia plate boundary from focal mechanisms and GPS data. Geophys J Int 169:1180–1200

Sherif MA, Kamal A, Naif AO (2020) Tectonic stress regime and stress patterns from the inversion of earthquake focal mechanisms in NW Himalaya and surrounding regions. J King Saud Univ Sci 33(2)

Snoke JA, Munsey JW, Teague AG, Bollinger GA (1984) A program for focal mechanism determination by combined use of polarity and SV-P amplitude ratio data. Earthq Notes 5(2):165–171

Spieker S, Wölbern I, Thomas C, Harnafi M, El Moudnib L (2014) Crustal and upper-mantle structure beneath the western Atlas Mountains in SW Morocco derived from receiver functions. Geophys J Int 198(3):1474–1485

Stich D, Serpelloni E, Mancilla F, Morales J (2006) Kinematics of the Iberia-Maghreb plate contact from seismic moment tensors and GPS observations. Tectonophysics 426(3–4):295–317

Stich D, Martín R, Morales J (2010) Moment tensor inversion for Iberia-Maghreb earthquakes 2005–2008. Tectonophysics 483:390–398

Teixell A, Arboleya ML, Julivert M, Charroud M (2003) Tectonic shortening and topography in the central high Atlas (Morocco). Tectonics 22(5):1051

Timoulali Y, Bouiflane M, Bouskri G, Azguet R, El Fellah Y (2019) Lithosphere structures dynamics in the central high Atlas (Morocco) by seismic tomography and gravimetric data. Geodesy Geodyn 10(3):241–255

Vavryčuk V (2011) Principal earthquakes: theory and observations for the 2008 West Bohemia swarm. Earth Planet Sci Lett 305(3–4):290–296

Vavryčuk V (2014) Iterative joint inversion for stress and fault orientations from focal mechanisms. Geophys J Int 199(1):69–77. https://doi.org/10.1093/gji/ggu224

Vernant P, Fadil A, Mourabit T, Ouazar D, Koulali A, Martin Davila J, Garate J, McClusky S, Reilinger R (2010) Geodetic constraints on active tectonics of the western Mediterranean: implications for the kinematics and dynamics of the Nubia- Eurasia plate boundary zone. J Geod 49:123–129

Wessel P, Smith WHF (1998) New improved version of the generic mapping tools released. EOS Trans Am Geophys Union 79(47):579